Supramolecular Architecture

Synthetic Control in Thin Films and Solids

Thomas Bein, EDITOR
Purdue University

Developed from a symposium sponsored
by the Division of Inorganic Chemistry
at the 201st National Meeting
of the American Chemical Society,
Atlanta, Georgia,
April 14–19, 1991

Contents

INDEXES

x

Chapter 20

Zeolite Inclusion Chemistry

Clusters, Quantum Dots, and Polymers

Thomas Bein

Department of Chemistry, Purdue University, West Lafayette, IN 47907

An overview on zeolite structures and properties is given, followed by a discussion of various strategies for the intrazeolite encapsulation of metal clusters and organometallics, quantum size semiconductor clusters, and polymer filaments. Several examples are described in more detail. Palladium clusters of low nuclearity have been prepared in the cavities of X zeolites via ion exchange with $Pd(NH_3)_4Cl_2$, oxidative dehydration, and subsequent reduction of the dry Pd(II)zeolites with hydrogen at 295 K. EXAFS analysis of Pd K-edge data shows that intrazeolite Pd_{2-4} clusters are formed by partial occupation of SI' and SII' positions of the sodalite subunits of the zeolite. Ensembles of CdSe have been synthesized within the cage system of zeolite Y via ion exchange with Cd(II) and subsequent treatment with H_2Se. Se,O bridged cadmium dimers and Cd_4O_4 cubes are formed in the sodalite unit. The anchoring chemistry of $Me_3SnMn(CO)_5$ in acid forms of zeolite Y was studied with X-ray absorption spectroscopy (Sn, Mn edge EXAFS) and in-situ FTIR/TPD-MS techniques. The compound attaches to the zeolite framework at the oxygen rings of the supercage. The attachment of the molecule occurs through the Sn moiety by loss of CH_4 gas while the Sn-Mn bond and the CO ligand sphere are still intact. Different degrees of substitution of the methyl groups by the acidic oxygen framework are observed. Intrazeolite polyacrylonitrile (PAN) was formed from preadsorbed acrylonitrile in zeolite Y and mordenite on reaction with radical initiators. Chain length analysis with gel permeation chromatography revealed a peak molecular weight of 19,000 for PAN in NaY, and about 1,000 for the polymer in mordenite. When intrazeolite PAN is pyrolyzed under nitrogen, black encapsulated material results that has lost the nitrile groups and hydrogen. After recovery from the zeolite hosts, the pyrolyzed polyacrylonitrile shows electronic DC conductivity at the order of 10^{-5} Scm^{-1}.

Zeolites Inclusion Chemistry: Structure and Properties of the Host

Few classes of inorganic solids have gained as much importance for host/guest chemistry as the microporous aluminosilicates called zeolites.[1,2,3] While many layered materials are known, including aluminosilicate clays, group 4 phosphates, graphite,

and metal chalcogenides, zeolites are the archetypical three-dimensional "molecular sieves". One major difference between these materials is that structural integrity of the zeolites upon encapsulation or intercalation of guest molecules is maintained, while the layered structures change the interlayer spacing and interlayer orientation when intercalation takes place. There are several other groups of crystalline microporous structures of growing importance, for example molybdenum phosphates,[4] or metal sulfides,[5] which are not subject of this discussion.

Zeolites are open framework oxide structures (classically aluminosilicates with hydrophilic surfaces) with pore sizes between 0.3 and 1.2 nm and exchangeable cations. The fundamental building blocks of the classical zeolite structure are the SiO_4 and AlO_4 tetrahedra that are conceptually viewed as joining up in "secondary building units" such as single six-rings (S6R, which are in fact twelve-rings consisting of six metals and six alternating oxygens arranged much like a crown ether), double-six-rings (D6R) and complex 5-1 structures. Other important structural units are the "sodalite cage" (a truncated octahedron) and the "supercage" (a unit with 12.5 Å internal diameter). These units are then joined to form open pore structures with channels based on rings containing 6 to 20 (in a gallophosphate) metal and oxygen atoms. Not only channels but also cage structures can be formed. There are now more than seventy different structure types known and new ones continue to emerge. Zeolites have remarkable temperature stability; survival of structures at 1000 K is not uncommon. The presence of Al atoms in the silica framework results in one negative charge per Al atom such that cations are required to balance the charge. The zeolitic pores constitute a significant fraction of the crystal volume (up to about 50%) and are usually filled with water. In hydrated zeolites, the cations have a high mobility giving rise to ion exchange capability, and the water molecules can be removed at elevated temperature. A general formula for zeolite-type materials based on 4-connected networks is the following[6]:

$$M_x M'_y N_z [T_m T'_n .. O_{2(m+n+..)-e} (OH)_{2e}](aq)_p \cdot qQ$$
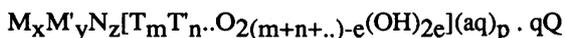
with tetrahedral T-atoms Be, B, Al, Ga, Si, Ge, P, transition metals, and M, M' exchangeable and nonexchangeable cations, N nonmetallic cations (normally removable on heating), (aq) chemically bonded water and Q sorbate molecules which need not be water. The essential part in the square brackets represents the 4-connected framework which is usually anionic. A simpler formula used for many zeolites is:

$$(M^{n+})_{x/n} [(AlO_2)_x (SiO_2)_y] \cdot zH_2O$$
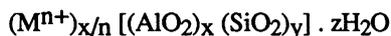
Structures of representative zeolites.[7] The following Table 1 presents a brief description of important zeolite structure types. Structural building blocks and cage topologies of those zeolites are shown in Figure 1. Zeolite A (LTA) consists of cubooctahedra (sodalite cages) linked together through double four-rings (D4R) to form a central cage (alpha-cage), accessible through six S8R with a free diameter of 4.1 Å.

Zeolite Y is isostructural with zeolite X (FAU). It differs from the latter in its higher Si/Al ratio which reduces the number of cations present in the framework. Zeolite X contains typically about 88 cations per unit cell, while Y contains about 56. The framework consists of sodalite cages, connected through four D6R that enclose a supercage with 12.5Å internal diameter. The supercages are accessible through four S12R windows with a free aperture of 7.4Å. Relevant cation locations are the center of the hexagonal prism (site SI) and in the six-membered rings connecting into the sodalite (SI'; SII') and into the supercage (SII). The ions are often slightly displaced from the center plane of the rings.

In mordenite (MOR), complex 5-1 units form two major intersecting channels, one defined by windows with oxygen 12-rings (6.5Å x 7.0Å) and one defined by windows with oxygen 8-rings. Mordenite is thermally very stable due to the large number of energetically favored five-membered rings in the framework.

Silicalite (MFI), $Si_{96}O_{192}$, belongs to the pentasil family of which the isostructural ZSM-5 is the most prominent. It has two intersecting pore systems, one consisting of zig-zag channels of near-circular cross section (5.3 x 5.6 Å) and another of straight channels of elliptical shape (5.1 x 5.5 Å) perpendicular to the first. All the intersections in silicalite are of the same size. The heat of adsorption and the room temperature uptake of water is small compared to the Al-containing zeolites.

Table 1. Representative Zeolite Structure Types.

Name	Unit Cell/Composition	Cage Type	Main Channels/Å[a]
LTA, Linde A	$Na_{12}[(AlO_2)_{12}(SiO_2)_{12}]$ 27 H_2O	a, β	4.1 ***
FAU, Faujasite	$Na_{58}[(AlO_2)_{58}(SiO_2)_{134}]$ 240 H_2O	β, 26-hedron(II)	7.4 ***
RHO, Rho	$Na_{12}[(AlO_2)_{12}(SiO_2)_{36}]$ 44 H_2O	a, D8R	3.9x5.1 ***
MOR, Mordenite	$Na_8[(AlO_2)_8(SiO_2)_{40}]$ 24 H_2O	complex 5-1	6.5x7.0* <-> 2.6x5.7*
MFI, ZSM-5	$Na_n[(AlO_2)_n(SiO_2)_{96-n}]$ 16 H_2O	complex 5-1	{5.3x5.6 <-> 5.1x5.5) ***
AFI, AlPO-5	$AlPO_4$	12R	7.3 *

[a] The number of stars (*) at the channel description indicates the dimensionality of channel connections. The cage types are depicted in Figure 1.

Zeolite synthesis.[8] A typical synthesis involves an aluminosilicate gel prepared from silicate and aluminate sources, hydroxide, and water, which is crystallized under hydrothermal conditions. Many zeolite preparations also contain organic cations such as tetramethyl ammonium hydroxide.[9] The organic cations are thought to be structure-directing templates, at least to a certain degree, because their presence changes the resulting zeolite phase and because they are often incorporated in the pores during synthesis. For example, tetrapropylammonium (TPA) ions are sited at the intersections of four channels in ZSM-5 with each of the four propyl groups directed along individual channels.[10] The SiO_2/Al_2O_3 ratio in these gels influences the final framework composition of the product, and usually all the aluminium available is incorporated into the final zeolite composition. The H_2O/SiO_2 and OH^-/SiO_2 ratios strongly influence the nature of the polymeric species present, and the rate of conversion of these species to three-dimensional zeolite frameworks.

Adsorption and acidity in zeolites. Intrazeolite water can be removed from the pores by heating and/or evacuating, resulting in a large, accessible intracrystalline surface area. Access of other species is limited to molecules having effective diameters small enough to enter the pores. However, the zeolite framework has a certain flexibility such that the pore size expands at elevated temperature. A classical example is the exclusion of nitrogen in NaA zeolite at cryogenic temperature (77 K), while at 180 K, the windows have expanded enough to adsorb 5 molecules of nitrogen in each cage. Other important factors influencing adsorption are polarizability of the adsorbate, wettability of the zeolite surface, and electric field gradients near cations. Zeolites
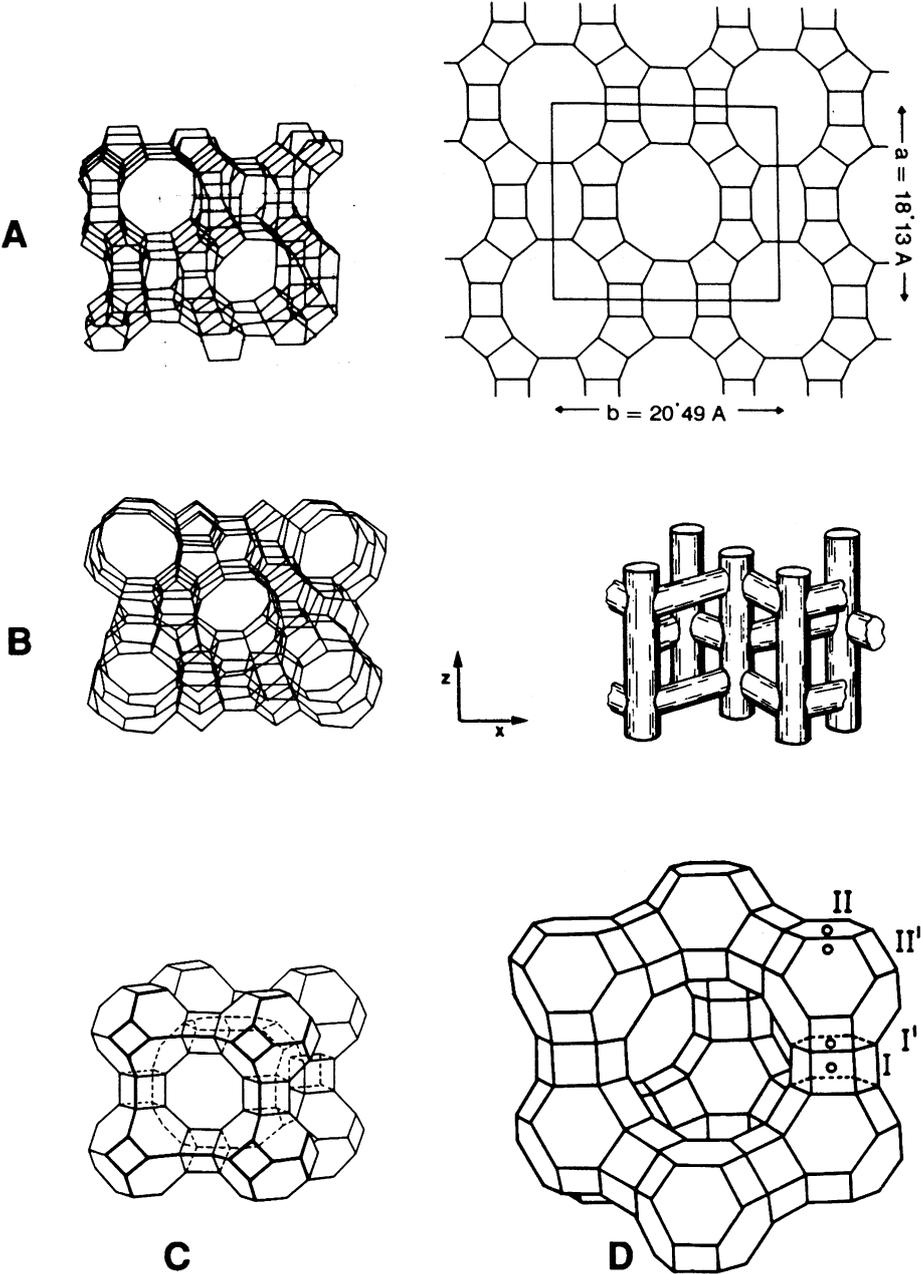
Figure 1.   The structures of zeolites. A, Mordenite, B, Silicalite, C, zeolite A, and D, Faujasite.

exhibit type I adsorption isotherms, where the initial rise at low partial pressure is associated with micropore filling.

Moderate acid will replace the original cations by hydronium ions;[11] the material can be heated to form hydrogen zeolites:

$$H_3O^+ZO^- \rightarrow H^+ZO^- + H_2O$$
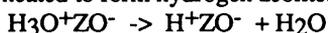
Bronsted acidity can also be introduced by hydrolysis of hydrated transition metal ions, and ammonium exchange with subsequent removal of ammonia under heating.[12]

The variety of zeolites and zeolite-related materials has grown enormously in recent years with the incorporation of transition metals into the framework,[13] and the discovery of metal aluminophosphate sieves.[14] Structural analogs to the zeolites as well as new structures with $AlPO_4$ elemental composition[15] include one example with a pore size greater than that of zeolite Y (VPI-5, pore size ~ 12Å).[16] Silicon has been incorporated into many of the $AlPO_4$ structures resulting in negatively charged frameworks.[17] New developments include the titanosilicates[18] containing octahedral Ti and the gallophosphate "cloverite" with impressive clover-like channels formed by 20-membered rings.[19]

Zeolites Inclusion Chemistry: Encapsulation Strategies

The crystalline microporosity and well-defined internal surfaces of zeolites, in addition to their great chemical variety, make these materials very attractive hosts for many areas of inclusion chemistry.[20] A brief overview of encapsulation strategies follows.

The two most obvious and common ways to incorporate matter into zeolite pores are (i) by adsorption and diffusion from gas or liquid phase, and (ii) by ion exchange. A third, usually more difficult approach involves incorporation of species during hydrothermal synthesis. The zeolite pores can be viewed as nanometer size reaction chambers that accommodate numerous organic and inorganic molecules with enough space for chemical conversions. It follows that there is a vast potential for ingenious chemistry in these hosts.

Supported metal clusters are important for catalytic applications and have therefore attracted attention for many years. Noble metals have been introduced into zeolites by ion exchange of complex cations such as $Pd(NH_3)_4^{2+}$. Degassing in oxygen eliminates premature autoreduction,[21] and subsequent hydrogen reduction forms very small metal clusters stabilized by the zeolite structure. (see example of Pd zeolites below). Other, more powerful reducing agents including H-atoms and sodium vapor have been used for metals such as Ni or Fe. Often a particle size distribution with additional external phase is obtained.

Metals can also be introduced by adsorption of the elemental vapor or melt, for instance in the case of mercury or alkali metals. Adsorption of molecular "precursors" such as carbonyls of iron, cobalt, nickel and molybdenum, and subsequent thermal or photochemical decomposition has become an important approach for metals that are difficult to reduce. Other ligands such as alkyls or acetylacetonates have also been used for this purpose. In all these cases, thermal decomposition carries the risk of excessive mobility of the precursors or intermediates such that agglomeration and particle formation at the external surface of the zeolite crystals can occur. Barrer has described the synthesis of salt-bearing zeolites including the famous dry synthesis of ultramarin in 1828, which is sodalite containing intercalated Na-polysulphides.[22] Adsorption of numerous non-ionic and salt species into zeolites was also described, either as such or as precursors for oxides, hydroxides, or metals.

Examples in four different areas of zeolite inclusion chemistry will be discussed in the following. Noble metal and semiconductor clusters, organometallics, and intrazeolite polymer filaments are objects of new and continued research activity.

Palladium Ensembles in Zeolites. Small metal particles or clusters have attracted great interest during the last decade. The optical, electronic and catalytic characteristics of clusters are expected to change from 'bulk' properties to 'molecular' properties within a certain size-range.[23,24] This change is represented by the transition of the electronic band structure of a crystal to the molecular orbital levels of species few atoms in size. Since the cluster size determines the relative population of coordination sites[25] and possibly its molecular symmetry, it is thought to be responsible for modified selectivities in a number of catalytic reactions.[26] Controlled synthesis of stable clusters with defined size is of particular interest, because this would potentially allow to fine-tune the properties of electronic materials and catalyst systems.

The particle size of Pd and Pt phases encapsulated in zeolite hosts can be controlled by chosing appropriate reduction conditions for the ion exchanged, dehydrated precursor form.[27,28,29] Based on x-ray diffraction studies, a bidisperse distribution of Pd particles appears to be typical: In addition to particles 10-20 Å in size, a second Pd phase was assigned to Pd atoms in the cage systems.[30,31] In the following we describe the synthesis and characterization of Pd ensembles, consisting of 2 to 4 correlated atoms, which are stabilized at room temperature in an open, chemically accessible zeolite matrix.[32] Characterization of the clusters was done by means of x-ray absorption spectroscopy (EXAFS).[33,34]

$Pd(NH_3)_4^{2+}$ was ion exchanged into zeolite NaX. Fourier transformed EXAFS data of Pd-X zeolite samples after different treatments are shown in Figure 2: after oxygen pretreatment at 625 K (PdXO, Figure 2.A); and after subsequent H_2 exposure at room temperature (PdX, Figure 2.B). In sample PdXO, the coordination of Pd^{2+} to oxygen with a Pd-O distance of 2.07 Å (1.5 Å uncorrected for phase shifts; fit results give the true distances) is detected as the main peak. This corresponds exactly to results from x-ray diffraction studies of similar palladium exchanged zeolites. The coordination of Pd to the zeolite is indicated in the EXAFS spectrum by the concomitant appearence of a peak at about 3.0 Å (uncorrected), typical for Si/Al scatterer of the zeolite framework.

If the sample PdXO is exposed to hydrogen at 295 K (PdX), drastic changes are visible in the corresponding EXAFS data. The data do not show any sign of remaining cationic Pd-zeolite-oxygen coordination between 1 to 2 Å, the range of the Pd-O contribution in sample PdXO. Instead, a very small, well-resolved contribution from Pd-Pd scattering is present. No outer palladium shells are visible, indicating an extremely small cluster size.

Analysis of the corresponding EXAFS data shows that under carefully chosen conditions it is possible to achieve a total reduction of zeolite-supported palladium cations to *metal clusters of molecular size at room temperature*. This is concluded from the fact that no remaining ionic Pd-oxygen coordination at the original distance of 2.07 Å (sample PdXO) is detected after reduction in sample PdX. A new, disordered Pd-O coordination at 2.76 Å in sample PdX is resulting from a weak interaction between the reduced metal atoms and the support which gives rise to an increased static disorder. Similar long metal-oxygen bond distances have been reported for a palladium phase in Y zeolites (Pd-O = 2.74 Å after H_2 reduction at 420 K)[22], and for silver clusters in zeolite Y (Ag-O = 2.67 and 2.79 Å after H_2 reduction at 348 K). The average coordination number of Pd-Pd in the zeolite is 1.5. This could point to the formation of dimeric and trimeric clusters. On average each Pd atom is surrounded by 3 oxygens and six Si/Al atoms.
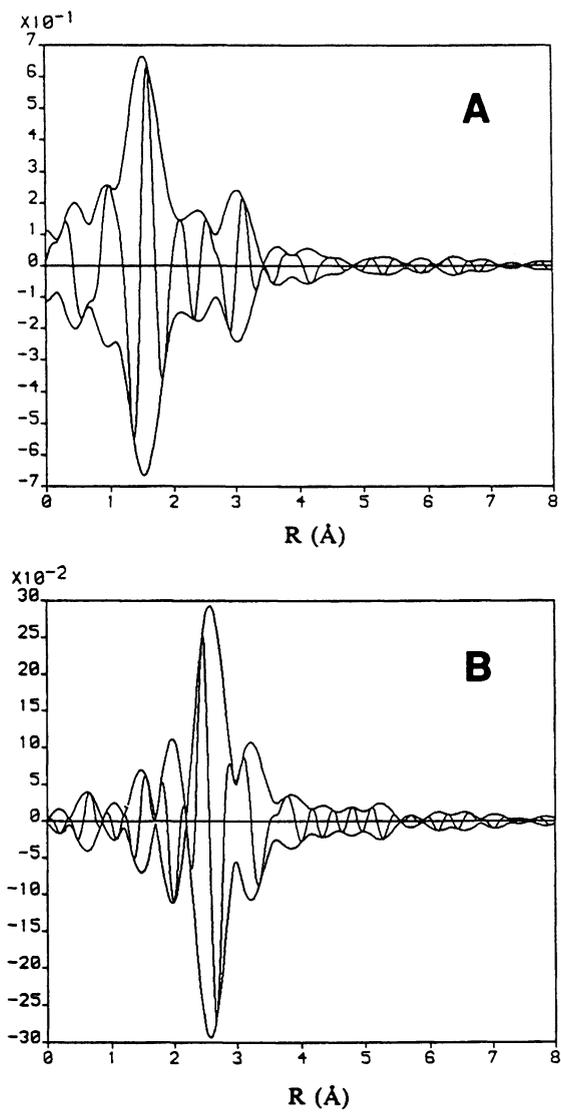
Figure 2. Fourier transformed EXAFS data of A, Sample PdXO; B, Sample PdX.

A model arrangement of four palladium atoms occupying the sodalite unit as shown in Figure 3 corresponds to an average Pd-Pd coordination of N = 1.5. Each palladium atom is located in front of one hexagonal window in dislocated SI' or SII' positions within the sodalite unit (SI'* and SII'*). The SI' sodalite position is surrounded by three nearest SII' positions and vice versa. Our proposed model of Pd$_2$ to Pd$_4$ molecular clusters is comparable to the structure of silver clusters in sodalite units, where the participating Ag atoms were located in SI'* and SII'* positions. Furthermore, x-ray diffraction studies of Ca(II)-exchanged and dehydrated zeolite Y and of Cd(II)-exchanged zeolites X were interpreted with very similar arrangements in SI'* positions, which are stabilized by OH or H$_2$O in SII' positions.[35,36]

The intrazeolite stabilization of the unusually small Pd clusters is possible through the interplay of two types of interaction: (1) The zeolite sodalite cage offers a stabilizing oxygen-coordination sphere for the reduced Pd atoms. (2) In addition, the different sets of SI'* and SII'* cage positions provide *templates* for the arrangement of palladium ensembles with sufficient Pd-Pd bonding overlap. These well-defined 'molecular clusters' with low nuclearity stabilized at ambient temperature in an open pore structure are attractive model systems to study changes in electronic, optical and vibrational characteristics, and to explore their catalytic properties under reaction conditions.

Quantum Size Cadmium Selenide Clusters in Zeolite Y. The preparation of well-defined semiconducting clusters with homogeneous morphology and size distribution is a prerequisite for understanding the physical origin of quantum size effects and exciton formation.[37,38,39] Classical preparation methods for these clusters include wet colloidal techniques,[40,41,42,43,44] and growth in dielectric glassy matrices,[45] or in polymers.[46] However, particle sizes obtained with these techniques are usually non-uniform and agglomeration of individual particles often occurs.[47] Zeolites are excellent hosts for nanometer size semiconductor clusters,[48] as demonstrated with Se species and CdS clusters.[49,50] A structural study of related cadmium selenide clusters stabilized in zeolite Y is discussed below.[51] Colloidal cadmium selenide is of interest for photosensitized electron-transfer reactions utilized for solar energy conversion and photocatalysis.[52,53,54]

Synthesis of intrazeolite CdSe was achieved by ion exchange with Cd(II), subsequent heating in oxygen to 673 K, and exposure to H$_2$Se gas at 298 K. Cluster size and geometrical arrangements could be determined by comprehensive analysis of Cd- and Se-edge EXAFS data as well as synchrotron x-ray powder diffraction and model calculations.

A comparison between EXAFS data of the cadmium-exchanged zeolite CdY and the samples treated with hydrogen selenide gas shows that major changes occur. From EXAFS data analysis and x-ray diffraction data of Cd(II) zeolite Y it was found that four Cd^{2+} ions occupy SI' cation positions in the sodalite cages, and that they are bridged by oxygen in adjacent SII' six-ring sites, thus forming small Cd$_4$O$_4$ cubes. On exposure to H$_2$Se it is expected that the selenium reacts with cadmium and the sample is expected to differ from the Cd(II) zeolite in its overall appearance primarily by an additional selenium shell. If the Fourier transforms of both samples are compared, a new peak at about 2.3 Å (uncorrected) in the CdSe-Y sample appears due to the selenide in this system. This assignment is further justified by the striking similarity in phase function and location in R-space to that of a reference sample of bulk CdSe.

X-ray powder data show that the Cd^{2+} in this sample is located primarily at SI'. This site, within the sodalite unit, is preferred by multivalent cations because some of the high charge density can be compensated by hydroxyl anions at SII', also in the sodalite unit. The cadmium at SI' has a pseudo octahedral coordination resulting from trigonal coordination to framework oxygens of the six-ring (which is part of the double
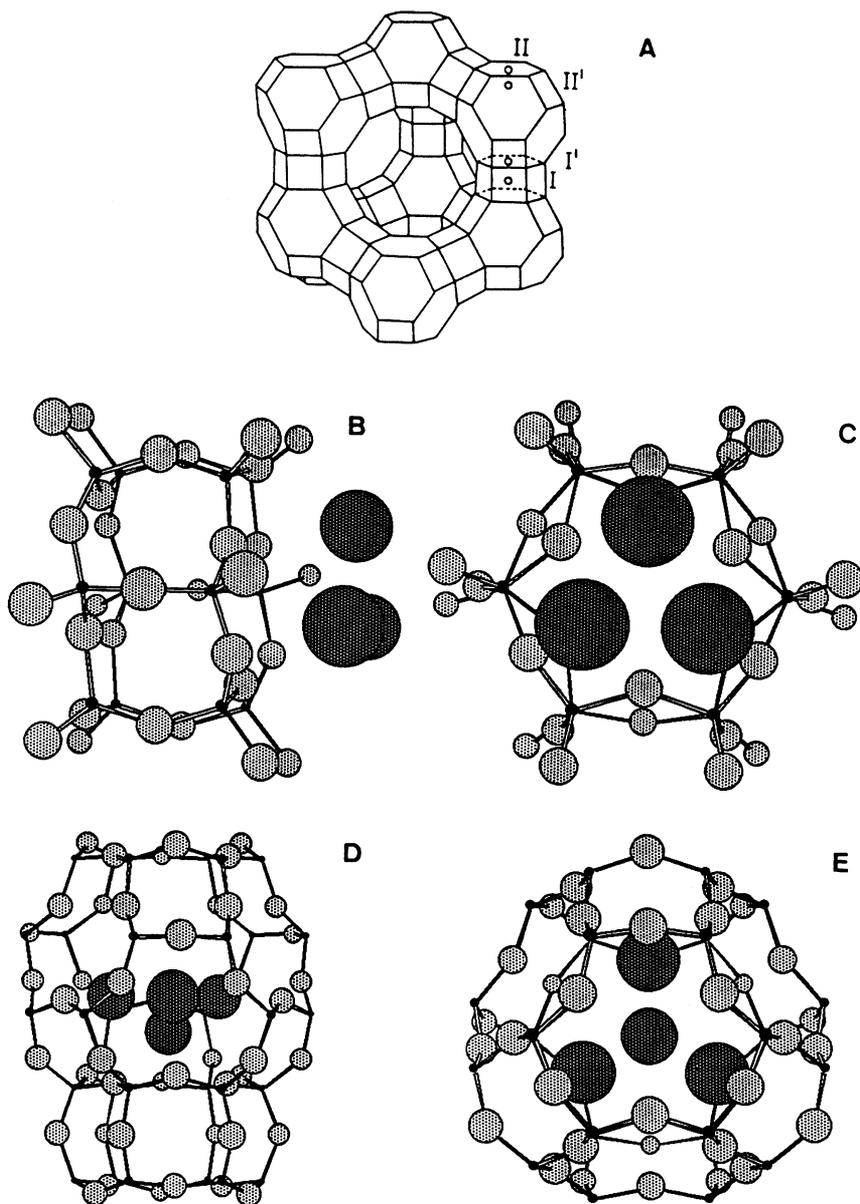
Figure 3.   Geometric arrangements of palladium ensembles in a faujasite subunit.
A: display of a partial faujasite unit cell with cation positions SI, SI', SII
and SII'. B,C: geometric arrangements of a palladium trimer located in
front of a double six-ring (side and top view; Pd atoms dark-shaded).
D,E: four Pd atoms located in adjacent SI' and SII' windows in a
sodalite cage. Radii of atoms are sized as follows: $Si^{4+} = 0.42$ Å , $O^{2-} =$
1.32 Å, $Pd(0) = 1.37$ Å. Si^{4+} and O^{2-} atoms are shown with 30% of
their ionic radii, $Pd(0)$ with 60% of its metallic radius.
From ref. 32. Copyright 1989 American Chemical Society.

six-ring interconnects of the zeolite Y structure) with a bond length of $Cd(1)-O(3) =$ 2.41 Å, and the three SII' atoms, $Cd(1)-O(5) = 2.42$ Å. $O(5)$ represents a site jointly occupied by Se and oxygen and hence the $Cd(1)-O(5)$ bond length is a weighted average of Cd-O (EXAFS data: 2.26 Å) and Cd-Se (EXAFS data: 2.60 Å).

In the CdSe-Y sample, the major fraction is composed of cadmium cations in adjacent SI' positions bridged on average by two extra-framework oxygen in SII' sites and one additional selenium ion in SII' sites. The second phase consists of Cd ions, present in the twelve-ring windows of the large cavities (SIII) coordinated to extra framework oxygen and one selenium.

The EXAFS-derived coordination number for Cd-O(5) at 2.26 Å is about half of that expected for a complete cube arrangement (expected for 70% Cd located in sodalite cage: $N = 3 \times 0.7 = 2.1$; found: $N = 1.4$). In addition, the small Cd-Cd interaction ($N = 0.4$) is not sufficient to account for a complete cube arrangement According to the XRD results, the cadmium cations are located in SI' and the O^{2-} ions in SII' positions. This indicates the formation of oxygen-bridged dimers Cd_2O_2. Based on the form factor for oxygen, the occupancy per unit cell was calculated to be 28.9. Since Cd_2O_2 dimers would account for only 11.4 oxygens, the remainder is assigned to selenium ions (0.4 Se per sodalite cadmium), detected by EXAFS with a bond distance Cd-Se of 2.60 Å. Thus, on average the sodalite units contain two cadmium ions occupying SI' positions, bridged by two oxygen in SII'. An additional selenium atom in SII' is bound to one cadmium atom (see Figure 4). This arrangement can be considered as a modified fragment of the Cd_4O_4 cube found in CdY zeolite.

The formation of Cd-Se ensembles in sodalite subunits must involve diffusion of H_2Se from the supercage through zeolite six-ring windows with a typical pore opening of 2.6 Å. The diameter of H_2Se (2.34 Å) clearly allows the diffusion to take place. The intrazeolite Cd-Se bond distance derived from this study is close to that of bulk CdSe and indicates some covalent character of these species. It is likely that HSe^- fragments replace the original (O5) species in the precursor $Cd_4(O)_4$ cube arrangement, forming Cd_2O_2Se fragments occupying the sodalite units. Additional CdO_2Se fragments at SIII positions are also detected. Non-coordinated helical selenium chains and a small fraction of CdSe are formed primarily in samples with a higher Se/Cd ratio.

Reactivity of Trimethyltin Manganesepentacarbonyl in Zeolite Cavities.

The immobilization of organometallic catalysts on heterogeneous supports has attracted growing attention,[55,56,57] because the high selectivity of many molecular catalysts[58] could be combined with the facile product separation and catalyst recovery inherent to heterogeneous systems. Zeolite hosts might offer additional features such as diffusional or transition state selectivity. Different strategies for the deposition of catalytically active organometallics into zeolites include physisorption of neutral metal carbonyls with only weak framework interactions,[59,60,61,62,63] diffusional blocking ("ship in the bottle" concept) of phthalocyanine (Pc) and other chelate complexes,[64,65,66] and ligation at transition metal cations. Intrazeolite Ru,[67] Ir,[68] and particularly Rh carbonyl complex cations have been studied in great detail.[69,70,71] Migration of intrazeolite Rh-carbonyl species and eventual formation of extrazeolite Rh(0) particles appears to occur under experimental conditions used for catalytic hydroformylation reactions[72].

Higher stability of the intrazeolite species should be expected from surface-attached complexes that utilize the bridging zeolite hydroxyls for anchoring reactions, such as the reaction of $Rh(allyl)_3$ with partially proton-exchanged X and Y type zeolite.[73,74,75,76]

Immobilization concepts for organometallic fragments in microporous solids are being developed in this laboratory. If two metal centers are present as in
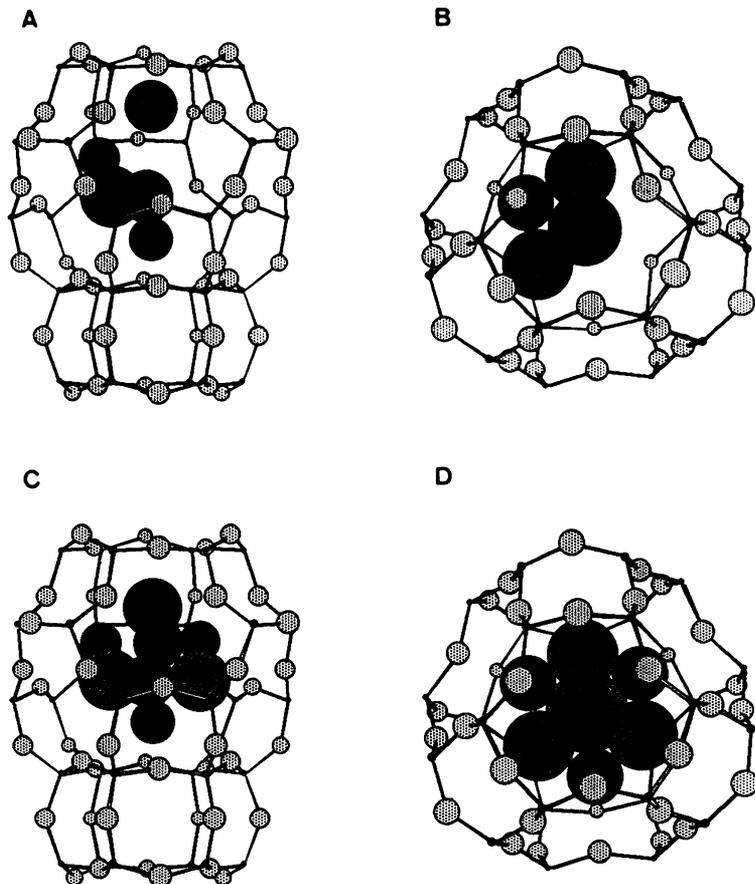
Figure 4.   Geometric arrangements of cadmium selenide species in a sodalite
                 subunit of the zeolite framework, viewed from the side and from top.
                 Framework oxygens: light shaded, extra framework oxygens: dark
                 striped, Cd cations black, Se atom light dotted.
                 Radii R = 1.32 Å for O^{2-}, R = 0.97 for Cd^{2+}, R = 1.17 for covalent Se.
                 A, B: $Cd(O_2)CdSe$ bridged fragment.
                 C, D: Cd_4O_4 cube. One sodalite unit incorporating the Cd moieties and
                 one of the four interconnecting double six rings of the faujasite
                 framework are presented. All framework atoms are sized 25% of their
                 radii. For clarity, the cube ensembles are shown with 75% of the radii.
                 From ref. 51. Copyright 1989 American Chemical Society.

heterobimetallic complexes, the complex can be 'anchored' to the support via one appropriately chosen, oxophilic metal, whereas the catalytic reaction may proceed at the second metal center. We could recently demonstrate the new bimetallic approach by utilizing the intrazeolite attachment chemistry of Ge-transition metal complexes.[77] Framework attachment of $Cl_2(THF)GeMo(CO)_5$ and $Cl_2(THF)GeW(CO)_5$ was possible in both the Na form of zeolite Y and in the proton-exchanged form. Both compounds react with the acidic zeolite at elevated temperatures under removal of chloride ligands.

As a recent example, we discuss the surface chemistry and stability of $Me_3SnMn(CO)_5$ in similar zeolite supports.[78] The precursor is expected to react with the internal surface hydroxyl groups of the zeolites by loss of methane gas whereas the Sn-Mn bond and the coordination sphere of Mn should remain intact. EXAFS and in situ FTIR data were used to characterize these systems.

EXAFS: Mn-absorption edge. After adsorption of 0.5 complexes $Me_3SnMn(CO)_5$ per supercage from hexane at room temperature into acidic Y zeolite, a full carbonyl coordination shell remained at the Mn atom: 5.2 carbon atoms at 1.87 Å and 6.0 oxygen atoms (Sn backscattering included) at 2.98 Å. At 373 K, the carbonyl coordination remains stable with 4.9 carbon atoms and 6.4 oxygen atoms (Sn modulation included) at 1.84 and 2.97 Å, respectively. At 423 K, dramatic changes are observed. The carbon and oxygen shells of the CO ligands have disappeared. The EXAFS data indicate the formation of small Mn clusters with Mn-Mn distances between about 2.4 and 3.7 Å. At 523 K, the Fourier transform presents a Mn-O bond as a first shell (N = 3.4 atoms, and R = 2.21 Å) and Mn-Si as an outer shell (N = 4.7 atoms, and R = 3.37 Å).

EXAFS: Sn-absorption edge. Fit results of the data of the intrazeolite precursor at 298 K, stripped of the Sn-Si shell show 2.4 atoms of C or O at 2.13 Å and the Sn-Mn bond at 2.56 Å (N = 1.2 atoms). The Sn-Mn bond length shrinks significantly compared to the Sn-Mn bond of the precursor. This effect was also found for the Sn-Mn bond (average distance = 2.59 Å) in $Cl_3SnMn(CO)_5$[79]. Most likely, the replacement of methyl groups by electronegative ligands increases electron density for the Sn-Mn π interaction by decreasing π back-bonding in the Mn-C bonds. This is also supported by the elongated Mn-CO distance in this sample (1.83 Å in NaY versus 1.87 Å in the acidic Y at RT).

From combined EXAFS, FTIR, TPD-MS and separate MS results of $Me_3SnMn(CO)_5$ in acidic Y zeolite, conclusions can be drawn as shown in Figure 5. Already at room temperature, the compound attaches to the zeolite framework at the oxygen rings of the supercage. The attachment of the molecule occurs through the Sn moiety by loss of CH_4 gas while the Sn-Mn bond and the CO ligand sphere are still intact. The substitution of methyl ligands by the oxygen atoms of the zeolite framework is supported by the EXAFS results which indicate that the electronegative oxygen atoms increase the Sn-Mn bond strength of the attached precursor in acidic Y zeolite. The resulting weakened Mn-CO interaction is confirmed by the higher CO-stretching frequencies of the precursor in acidic Y. Based on IR data, both mono- and di-substitution of methyl groups by the framework oxygen atoms occurs. The mono-substituted species, $(Oz)Me_2SnMn(CO)_5$, is the major product at room temperature while the di-substituted species, $(Oz)_2MeSnMn(CO)_5$, is formed at higher temperature, *ca.* 373 K. The attached species decompose at 423 K by loss of CO ligands and cleavage of the Sn-Mn bond. One methyl ligand remains on the zeolite-attached tin atom. Unidentified Mn species are left inside the zeolite cavities as a result of the decomposition.

These results show that the heterobimetallic compound $Me_3SnMn(CO)_5$ can be anchored into the cages of acidic zeolites at room temperature under retention of the Sn-Mn bond. The methyl ligands are good leaving groups in acidic Y but do not react in
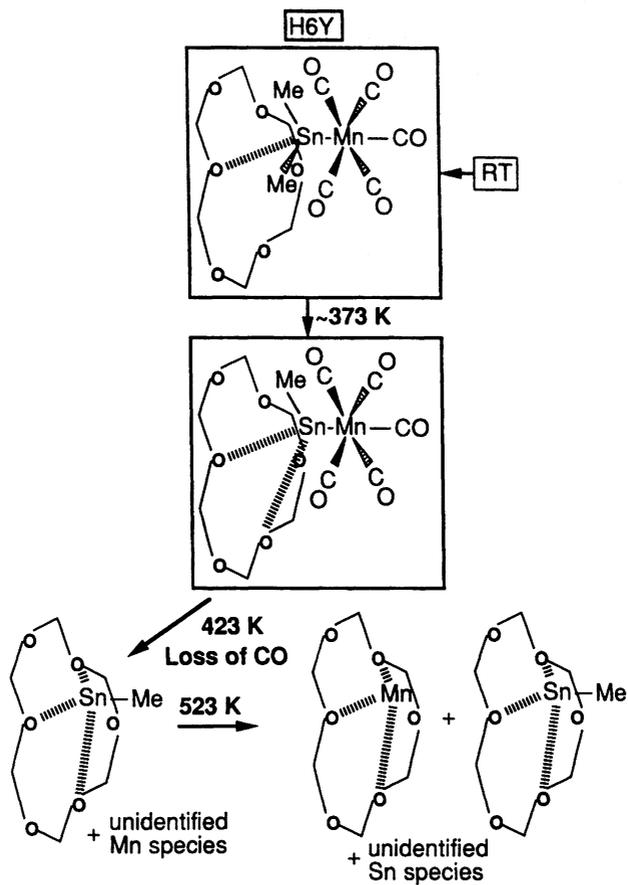
Figure 5.   The chemistry of Me₃SnMn(CO)₅ in acid Y zeolite.

NaY. The thermal stability of the intrazeolite, attached species permits further studies on their chemical reactivity and potential catalytic activity.

Polyacrylonitrile Chains in Zeolite Channels: Polymerization and Pyrolysis. The quest for ever smaller and faster devices for information processing aims at the control of electronic conductivity at nanometer dimensions. Conducting organic polymers are interesting candidates for this purpose. Studies of the conduction mechanism of conjugated polymers[80,81,82,83,84] would benefit substantially if the low-dimensional structures were available as decoupled, structurally well-defined entities. We have recently demonstrated the encapsulation of conjugated polymers such as polypyrrole, polyaniline and polythiophene in zeolite channels.[85] Precursor monomers are introduced into the zeolite host and are subsequently polymerized by appropriate oxidants in the pore system. Methylacetylene gas reacts with the acid sites in zeolites L, Y, and others to form reactive, conjugated oligomers.[86] Short-chain oligomers of polythiophene were prepared, oxidatively doped to the conducting state and stabilized in Na-pentasil zeolites[87]. The synthesis of these and related systems is a step towards the design of oriented *"molecular wires"*, that could in principle permit to process signals or to store information inside channel systems with nanometer dimensions.

As a last example of zeolite inclusion chemistry, we discuss the assembly of polyacrylonitrile (PAN) strands in different large-pore zeolites, zeolite Y and mordenite, and explore the pyrolysis reactions of the encapsulated polymer (Figure 6).[88]

Acrylonitrile vapor was adsorbed in the degassed (670 K, 10^{-5} Torr) zeolite crystals at a vacuum line for 60 min at 298 K. To an aqueous suspension of the acrylonitrile-containing zeolite were added aqueous solutions of potassium peroxodisulfate and sodium bisulfite as radical polymerization initiators.[89] The zeolite frameworks could be dissolved with HF to recover the intrazeolite polyacrylonitrile (PAN). IR and NMR data show no damage to the polymers after this treatment. For pyrolysis, the zeolite/PAN adducts were heated under nitrogen or vacuum to 920 and 970 K for extended periods.

On saturation, zeolite Y contains 46 and mordenite 6 molecules of acrylonitrile per unit cell. The polymer recovered from the zeolite hosts is identical to bulk PAN as shown by NMR spectroscopy.[90] The ^{1}H NMR spectra show two bands at a ratio of 2 to 1, one at 2.0 ppm corresponding to the methylenic group in the polymer, and the other at 3.1 ppm confirming a methine group. The ^{13}C NMR data of the zeolite-extracted PAN show CH_2 (27.5 ppm), CH (32.7 ppm), and -CN (120.1 ppm), identical to the bulk material.

Infrared spectra of the zeolite/polymer inclusions and of PAN extracted from the zeolites show also peaks characteristic of the bulk polymer,[91,92] including methylenic C-H stretching vibrations of the backbone (2940 cm^{-1} and at 2869 cm^{-1}), and a band at 2240 cm^{-1} due to the pendant nitrile group. The spectra of the extracted intrazeolite polymers are indistinguishable from the spectrum of the bulk polymer. We conclude that the polymer formed in the zeolites is polyacrylonitrile.

Gel permeation chromatography was used to determine the molecular weight of the polymer extracted from the zeolites, relative to a PAN broad standard (M_w = 86,000; M_n = 23,000). For PAN extracted from NaY, the main molecular weight distribution peaks at 19,000, corresponding to 360 monomer units or about 0.2 μm for an extended chain. For PAN extracted from Na-mordenite, a bimodal molecular weight distribution is observed; a small fraction peaks at 19,000 and a large fraction at about 1,000, corresponsing to a 0.01 μm chain in a fully extended form. The shorter chain length in mordenite might indicate crystal defects or diffusional constraints for the polymerization reaction.
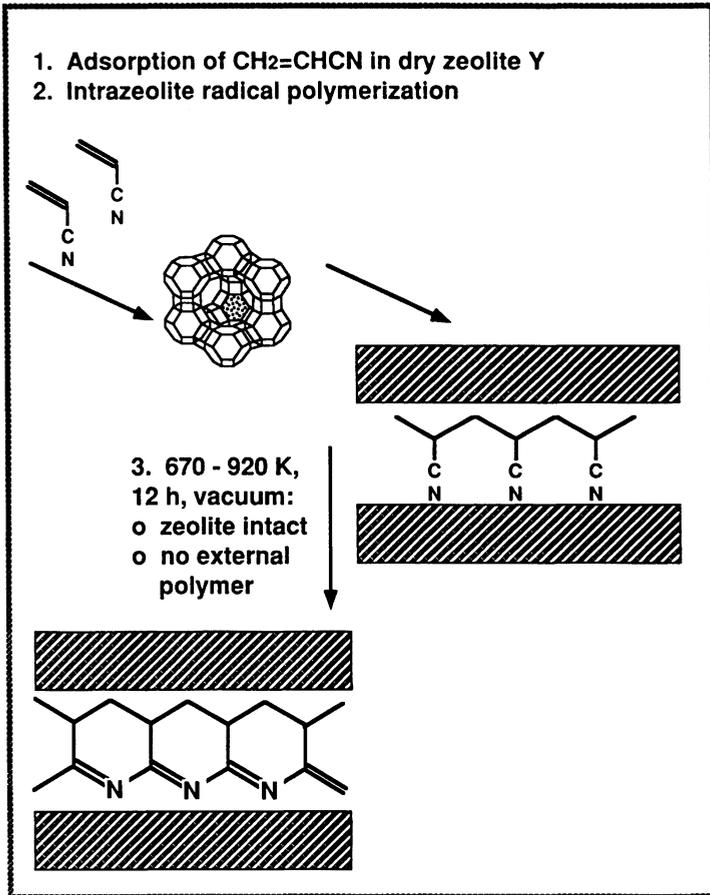
Figure 6.   Intrazeolite polymerization and tentative pyrolysis product of acrylonitrile.

Pyrolysis changes the color of the PAN-containing zeolites from white to grey-black.[93] The electronic absorption spectrum of pyrolyzed PAN extracted from NaY shows the appearance of a feature at about 350 nm, as in the bulk, probably due to conjugated carbon-nitrogen double bonds in the ladder polymer.[94] The rest of the spectrum is practically structureless and resembles the absorption spectrum of graphite. The methylenic stretching vibrations and the nitrile band of the intrazeolite PAN main chain disappear. New bands appear in the 1400-1600 cm^{-1} region which have been assigned to C=C and C=N double bonds in the pyrolyzed bulk PAN, as well as the tail of the electronic excitation corresponding to free carrier absorption. A sample of bulk PAN heated to 800 K instead of 920 K shows more defined features in the 1400-1600 cm^{-1} region, similar to the case of pyrolyzed PAN (920 K) extracted from the zeolite. This suggests an early stage of graphitization for the intrazeolitic material. Zeolite/PAN samples pyrolyzed at different temperatures, times, and atmospheres, (nitrogen or vacuum) show spectra similar to the spectrum of bulk PAN pyrolyzed to 800 K.

Samples of NaY with pyrolyzed (920 K) PAN show no measurable dc conductivity. This is not surprising because the polymer is encapsulated completely within the insulating zeolite, and because no external polymer coats the zeolite crystal surfaces. However, the conductivity of the pyrolyzed PAN *extracted* from the zeolite is at the order of 10^{-5} Scm^{-1}, almost identical with that of bulk PAN pyrolyzed at 800 K, and five orders of magnitude smaller than that of the bulk sample pyrolyzed at 920 K. In contrast to the bulk polymer, pyrolysis treatment conditions above about 870 K have little effect on the resulting conductivity of the extracted intrazeolite samples. We conclude that the spatial limitations within the zeolite channels prevent the formation of more extended, graphitized structures with higher conductivity.

This study demonstrates the inclusion synthesis of polyacrylonitrile in the channel systems of NaY and Na-mordenite zeolites, and its pyrolysis to yield a conducting material consisting of nanometer size carbon filaments. These and related systems are promising candidates for low-field conductivity at nanometer scale dimensions.

Conclusion. The examples discussed above demonstrate the versatility and great potential of zeolite molecular sieves to encapsulate and stabilize often unusual forms of matter. The zeolite pores form nanometer size reaction chambers that permit ready access to the external world via adsorption and ion exchange. The regular arrangement of the cages and their variable connectivity is of great interest for superlattice assembly of electronic and optical materials.

So far, research in this area has emphasized metal clusters, organometallics, and quantum size semiconductor clusters and superlattices. As experimental techniques become available, the dynamics of intrazeolite reactions, such as catalysis, ligand exchange,[95] electron transfer and radical reactions, and polymerizations will be explored in more detail. As molecular sieves with ever larger pores are being discovered, the future potential to assemble and understand supramolecular structures is enormous.

Literature cited

1   Breck, D.W. "Zeolite Molecular Sieves", R.E. Krieger Publishing Co., Malabar, FL,1984
2   "New Developments in Zeolite Science and Technology", Murakami, Y; Iijima, A; Ward, J.W., eds., Kodansha, Tokyo, 1986
3   R. Szostak, Molecular Sieves. Principles of Synthesis and Identification, Van Nostrand Reinhold, New York, 1989.
4   Haushalter, R. C.; Strohmaier, K. G.; Lai, F. W. Science 1989, 246, 1289
5   Bedard, R. L.; Wilson, St. T.; Vail, L. D.; Bennett, J. M.; Flanigen, E. M. Studies Surf. Science Catal. 49, Elsevier,1989, 375
6   Meier, W.M. "New Developments in Zeolite Science and Technology", Murakami, Y; Iijima, A; Ward, J.W., eds., Kodansha, Tokyo, 1986, 13
7   Atlas of Zeolite Structure Types. Meier, W. M.; Olson, D. H. 2nd Ed., Butterworths, London, 1987
8   (a) Barrer, R. M. "Hydrothermal Synthesis of Zeolites", Academic Press, London, 1982. (b) Szostak, R. "Molecular Sieves. Principles of Synthesis and Identification", Van Nostrand Reinhold, 1989
9   B. M. Lok, T. R. Cannan, and C. A. Messina, Zeolites, 1984, 4, 289.
10   R. J. Argauer, and G. R. Landolt, US Patent 3,702,886, 1972.
11   P. A. Jacobs, Carboniogenic Activity of Zeolites, Elsevier, Amsterdam, 1977.
12   J. W. Ward, J. Catal., 1968, 11, 238.
13   Ball, W.J.; Dwyer, J.; Garforth, A.A.; Smith, W.J. "New Developments in Zeolite Science and Technology", Murakami, Y; Iijima, A; Ward, J.W., eds., Kodansha, Tokyo, 1986, 137
14   Messina, C.A.; Lok, B.M.; Flanigen, E.M. U. S. Patent 4,544,143
15   S. T. Wilson, B. M. Lok, C. A. Messina, T. R. Cannan, and E. M. Flanigen, J. Am. Chem. Soc., 1982, 104, 1146.
16   M. E. Davis, C. Saldarriaga, C. Montes, J. Garces, and C. Crowder, Zeolites, 1988, 8, 362.
17   B. M. Lok, C. A. Messina, R. L. Patton, R. T. Gajek, T. R. Cannan, and E. M. Flanigen, J. Am. Chem. Soc., 1984, 106, 6092.
18   Chemical & Engineering News, Sept. 30, 1991, 31
19   Kessler, H. Mat. Res. Soc. Symp. Proc. Vol. 233, 1991, 47
20   (a) Ozin, G. A.; Kuperman, A.; Stein, A. Angew. Chem. Int. Ed. Engl., 1989, 28, 359. (b) Ozin, G. A.; Gil, C. Chem. Rev. 1989, 89, 1749.
21   Sachtler, W. H. M., Stud. Surf. Sci. Catal. 49, Elsevier, 1989, 975
22   Barrer, R. M. "Hydrothermal Synthesis of Zeolites", Academic Press, London, 1982, 306
23   "Contribution of Clusters Physics to Materials Science and Technology", Ed. Davenas, J., Rabette, P. M. ; NATO ASI Series, E104 ; Martinus Nijhoff: Dordrecht, 1986
24   "Metal Clusters", Ed. M. Moskovits; Wiley: New York, 1986
25   Van Hardeveld, R.; Hartog, F. Surf. Sci. 1969, 15, 189
26   Somorjai, G. A., in "Catalyst Design", Hegedus, L. L., Ed.; Wiley: New York, 1987, 11
27   Exner,D.; Jaeger, N.; Moller, K.; Schulz-Ekloff, G. J. Chem. Soc., Faraday Trans. 1, 1982, 78, 3537

28   Exner, D.; Jaeger, N.; Moller, K.; Nowak, R.; Schrubbers, H.; Schulz-Ekloff,
     G.; Ryder, P. Studies in Surf. Sci, Vol. 12, Ed. Jacobs, P.A.;
     Elsevier:Amsterdam, 1982, 205
29   Bergeret, G.; Gallezot, P.; Imelik, B. J. Phys. Chem. 1981, 85, 411
30   Gallezot, P.; Imelik, B. Adv. Chem. Ser. 1973, 121, 66
31   Bergeret. G.; Tran Manh Tri; Gallezot, P. J. Phys. Chem. 1983, 87, 1160
32   Moller, K.; Koningsberger, D. C.; Bein, T. J. Phys. Chem., 1989, 93, 6116
33   Teo, B. K. "EXAFS: Basic Principles and Data Analysis"; Springer: Berlin,
     1986
34   "X-Ray Absorption: Principles, Applications, Techniques of EXAFS,
     SEXAFS and XANES", Koningsberger, D. C.; Prins, R., Ed.; Wiley: New
     York, 1987
35   Costenoble, M. L.; Mortier, W. J.; Uytterhoeven, J. B. J. Chem. Soc.,
     Faraday Trans. 1 1978, 74, 466
36   Calligaris, M.; Nardin, G.; Randaccio, L.; Zangrando, E. Zeolites 1986, 6,
     439
37   Brus, L. J. Phys. Chem. 1986, 90, 2555
38   Nedeljkovic, J. M.; Nenadovic, M. T.; Micic, O. I.; Nozik, A. J. J. Phys.
     Chem. 1986, 90, 12
39   Nozik, A. J.; Williams, F.; Nenadovic, M. T.; Rahj, T.; Micic, O. I. J. Phys.
     Chem. 1985, 89, 397
40   Henglein, A. Ber. Bunsen Ges. Phys. Chem. 1984, 88, 969
41   Ramsden, J. J.; Webber, S. E.; Grätzel, M. J. Phys. Chem. 1985, 98, 2740
42   Dannhauser, T.; O'Neil, M.; Johansson, K.; Whitten, D.; McLendon, G. J.
     Phys. Chem. 1986, 90, 6074
43   Tricot, Y.-M.; Fendler, J. H. J. Phys. Chem. 1986, 90, 3369
44   Variano, B. F.;Hwang, D. M.; Sandroff, C. J.; Wiltzius, P.; Jing, T. W.; Ong,
     N. P. J. Phys. Chem. 1987, 91, 6455
45   Ekimov, A. I.;Efros, Al. L.; Onushchenko, A. A. Solid State Comm. 1985,
     921
46   Wang, Y.; Mahler, W. Opt. Comm. 1987, 61, 233
47   Chestnoy, N.; Hull, R.; Brus, L. E. J. Chem. Phys. 1986, 85, 2237
48   Stucky, G. D.; Mac Dougall, J. E. Science, 1990, 247, 669
49   Parise, J. B.; MacDougall, J. E.; Herron, N.; Farlee, R.; Sleight, A. W.;
     Wang, Y.; Bein, T.; Moller, K.; Moroney, L. M. Inorg. Chem. 1988, 27, 221
50   Herron, N.; Wang, Y.; Eddy, M.; Stucky, G. D.; Cox, D. E.; Moller, K.;
     Bein, T.; J. Am. Chem. Soc., 1989, 111, 530
51   Moller, K.; Eddy, M. M.; Stucky, G. D.; Herron, N.; Bein, T. J. Am. Chem.
     Soc., 1989, 111, 2564
52   Bard, A. J. J. Phys. Chem 1982, 86,172
53   Grätzel, M. Acc. Chem. Res. 1982, 15, 376
54   Darwent, J. R. J. Chem. Soc., Faraday Trans. 1 1984, 80, 183
55   Lamb, H. H.; Gates, B. C.; Knözinger, H. Angew. Chem. Int. Ed.
     Engl. 1988, 27, 1127
56   Basset, J.M.; Choplin, A J. Mol. Catal. 1983, 21, 95
57   Bailey, D.C.; Langer, S.H. Chem. Rev. 1981, 81, 109
58   Jardin, F.H. Prog. Inorg. Chem. 1981, 28, 63
59   Ballivet-Tkatchenko, D.; Coudurier, G.; Mozzanega, H.;
     Tkatchenko, I.; Kinnemann, A. J. Mol. Catal. 1979, 6, 293
60   Suib, S.L.; Kostapapas, A.; McMahon, K.C.; Baxter, J.C.; Winiecki,
     A.M. Inorg. Chem. 1985, 24, 858

61   Bein, T.; McLain, S.J.; Corbin, D.R.; Farlee, R.F.; Moller, K.;
      Stucky, G.D.; Woolery, G.; Sayers, D. J. Am. Chem. Soc. 1988,
      110, 1801
62   Bein, T.; Schmiester, G.; Jacobs, P.A. J. Phys. Chem. 1986, 90,
      4851
63   Yang, Y.S.; Howe, R.F. "New Developments in Zeolite Science and
      Technology", Murakami, Y.; Iijima, A.; Ward, J.W., eds., Kodansha, Tokyo,
      1986, 883
64   Herron, N. Inorg. Chem. 1986, 25, 4714
65   Diegruber, H.; Plath, P.J.; Schulz-Ekloff, G. J. Mol. Catal. 1984,
      24, 115
66   Herron, N.; Stucky, G.D.; Tolman, C.A. J.C.S., Chem. Comm.
      1986,521
67   Verdonck, J.J.; Schoonheydt, R.A.; Jacobs, P.A. J. Phys. Chem.
      1983, 87, 683
68   Gelin, P.; Naccache, C.; Ben Taarit, Y.; Diab, Y. Nouv. J. Chim.
      1984, 8, 675
69   Bergeret, G.; Gallezot, P.; Gelin, P.; Ben Taarit, Y.; Lefebvre, F.;
      Naccache, C.; Shannon, R.D. J. Catal. 1987, 104, 279
70   Davis, M.E.; Schnitzer, J.; Rossin, J.A.; Taylor, D.; Hanson, B.E.
      J. Mol. Catal. 1987, 39, 243
71   Shannon, R.D.; Vedrine, J.C.; Naccache, C.; Lefebvre, F. J. Catal.
      1984, 88, 431
72   Rode, E.J.; Davis, M.E.; Hanson, B.E. J. Catal. 1985, 96, 574
73   Huang, T.N.; Schwartz, J.; Kitajima, N. J. Mol. Catal. 1984, 22,
      38
74   Huang, T.N.; Schwartz, J. J. Am. Chem. Soc. 1982, 104, 5244
75   Corbin, D.R.; Seidel, W.C., Abrams, L.; Herron, N.; Stucky, G.D.;
      Tolman, C.A. Inorg. Chem. 1985, 24, 1800
76   Taylor, D. F.; Hanson, B. E.; Davis, M. E. Inorg. Chim. Acta 1987,
      128, 55
77   (a) Borvornwattananont, A.; Moller, K.; Bein, T. J. Chem. Soc.,
      Chem. Commun. 1990, 28. (b) Borvornwattananont, A.; Moller, K.;
      Bein, T., Synthesis/Characterization and Novel Applications of Molecular Sieve
      Materials, R. L. Bedard, T. Bein, M. E. Davis, J. Garces, V. A. Maroni, G.
      D. Stucky, Eds., Mat. Res. Soc. Symp. Proc. 233, 1991, p. 195.
      (c) Borvornwattananont, A.; Bein, T., submitted.
78   Borvornwattananont, A.; Bein, T., submitted.
79   Onaka, S., Bull. Chem. Soc. Japan, 1975, 48(1), 319.
80   Proceedings of the International Conference on Science and Technology of
      Synthetic Metals, ICSM '88 and '90; Synth. Metals 1988, 28 (1-3) and 29(1),
      and Synth. Metals 1991, 41-43.
81   Handbook of Conducting Polymers; T. A. Skotheim, Ed.; Marcel Dekker,
      New York, Vol. 1, 1986.
82   Conducting Polymers. Special Applications; L. Alcacer, Ed.; D. Reidel,
      Dordrecht , 1987.
83   Hopfield, J. J.; Onuchic, J. N.; Beratan, B. N. Science 1988, 241, 817
84   (a) Molecular Electronic Devices; F. L. Carter, Ed., Marcel Dekker, New
      York, 1982.
      (b) Molecular Electronic Devices II; F. L. Carter, Ed., Marcel Dekker, New
      York, 1987.
85   (a) Enzel, P.; Bein, T. J. Phys. Chem. 1989, 93 , 6270.

(b) Enzel, P.; Bein, T. J. Chem. Soc., Chem. Commun. 1989, 1326.

(c) Bein, T.; Enzel, P. Angew. Chem., Int. Ed. Engl. 1989, 28, 1692.

(d) Bein, T.; Enzel, P. Mol. Cryst. Liq. Cryst., 1990, 181, 315.

(e) Bein, T.; Enzel, P. ; Beuneu, F.; Zuppiroli, L.
"Inorganic Compounds with Unusual Properties III. Electron Transfer in Biology and the Solid State", M. K. Johnson et al., Eds., ACS Adv. Chem. Ser., No. 226, 1990, p. 433

86   Cox, S. D.; Stucky, G. D. J. Phys. Chem., 1991, 95, 710.

87   Caspar, J. V.; Ramamurthy, V.; Corbin, D. R. J. Am. Chem. Soc., 1991, 113,   600.

88   Enzel, P.; Bein, T., submitted.

89   At molar ratios acrylonitrile: peroxodisulfate: bisulfite of 1:0.0027:0.0035.

90   G. Svegliado, G. Talamini, and G. J. Vidotto, Polym. Sci. A-1, 1967, 5, 2875.

91   M. M. Coleman, and R. J. Petcavich, J. Polym. Sci. Phys. Ed., 1978, 16, 821.

92   T. -C. Chung, Y. Schlesinger, S. Etemad, A. G. MacDiarmid, and A. J. Heeger, J. Polym. Sci. Phys. Ed., 1984, 22, 1239.

93   X-ray powder diffraction data demonstrate that the zeolite framework remains intact even after pyrolysis treatments at 970 K for NaY. Scanning electron micrographs show no apparent external bulk polymer coating the zeolite crystals indicating that most of the polymer chains reside in the interior of the zeolite crystals.

94   C. L. Renschler, A. P. Sylwester, and L. V. Salgado, J. Mat. Res. 1989, 4, 452.

95   Ozin, G. A.; Özkar, S.; Pastore, H. O.; Poë, A. J.; Vichi, E. J. S. J. Chem. Soc., Chem. Commun., 1991, 141.